The GDH Sum Rule with Nearly-Real Photons and the Proton g_1 Structure Function at Low Momentum Transfer

M. Anghinolfi, M. Battaglieri (Co-spokesperson), R. De Vita (Co-spokesperson),
M. Osipenko, G. Ricco, M. Ripani (Spokesperson *), M. Taiuti
Istituto Nazionale di Fisica Nucleare, Via Dodecanneso 33, I-16146 Genova (Italy)

S. Simula
Istituto Nazionale di Fisica Nucleare, Via della Vasca Navale 84, I-00146 Roma (Italy)

E. Golovatch, E. Isupov, B. Ishkhanov, V. Mokeev
Nuclear Physics Institute, Moscow State University

G. Dodge, S. Kuhn
Old Dominion University, Norfolk, Virginia

W. Brooks, V. Burkert, L. Elouadrhiri
Thomas Jefferson National Accelerator Facility,
12000 Jefferson Avenue, Newport News, Virginia, 23606

K. Joo
University of Connecticut, Storrs, Connecticut

P. Bosted
University of Massachusetts, Amherst, Massachusetts

R. Minehart, L.C. Smith
University of Virginia, Charlottesville, Virginia

and the CLAS collaboration

Contents

*contact person: ripani@ge.infn.it

Abstract

We propose a measurement of the helicity-dependent inclusive cross section difference for scattering of longitudinally polarized electrons from polarized protons at $Q^2 = 0.01 - 0.5$ GeV^2, and in a large x (or W) range. We will use the Hall B polarized solid state target and a modified CLAS detector. This will allow to determine the generalized GDH integral. Systematic errors will be reduced compared to the usual method of measuring double polarization asymmetries. The results will put stringent constraints on different approaches in Chiral Perturbation Theory at small Q^2, as well as tests of phenomenological models aimed at describing the entire Q^2 range. The proposed Q^2 coverage will be achieved by operating CLAS with reversed torus magnet polarity, and inserting in one CLAS sector a new gas Cherenkov counter designed to optimize electron detection efficiency and pion rejection in these operating conditions. We propose to use four different energies to cover the W range from elastic scattering to W =2.1 GeV at least, without the necessity of interpolating between the data sets. The ability of CLAS to simultaneously measure the elastic process allows us to continuously monitor the product of beam and target polarization, and to check the normalization by extracting the unpolarized elastic cross section. The expected results will add high precision information on the nucleon spin response in kinematics where tests of low energy fundamental theories are possible, and provide the data for an improved understanding of hadronic spin processes in the domain of confinement. The experiment covers a kinematics similar to the Hall A measurements on the neutron (polarized ^{3}He).

1 Introduction

The study of hadronic structure with electromagnetic probes is deeply concerned with fundamental questions about the basic constituents of hadrons. In particular the spin structure of the nucleon which is one of the main topics in hadronic physics has been investigated for now more than three decades using lepton and photon beams. Measurements of the spin-dependent structure functions g_1 and g_2 have been performed at large Q^2 (Deep Inelastic Scattering region) at several facilities as SLAC, CERN, and DESY [1], providing information for the understanding of the nucleon structure in terms of the elementary constituents of QCD, i.e. quarks and gluons. On the contrary much less is known in the low momentum transfer region ($Q^2 < 1 - 2$ GeV^2), where non-perturbative phenomena as nucleon resonances start to play a dominant role. In this kinematic domain, perturbative techniques which have been successfully applied at high energy fail due to the growth of the strong coupling constant. Lattice gauge theories will hopefully provide the connections between composite hadrons and fundamental constituents in this regime. However presently phenomenological models are still the main tool for the description of the hadron properties.

At very low momentum transfer ($Q^2 < 0.05 - 0.1$ GeV^2), an alternative approach is given by Chiral Perturbation Theory (χPT) which provides an effective representation of the QCD Lagrangian based on hadronic degrees of freedom and can be considered as a fundamental theory in the low energy limit. χPT is nowadays a well developed theoretical tool capable of predicting the dynamics of hadronic processes in the non-perturbative regime and its test is important to identify the degrees of freedom which dominate in this kinematic domain.

A fundamental prediction concerning the spin structure of the nucleon in the non perturbative regime is the Gerasimov-Drell-Hearn sum rule [2, 3] which relates the helicity-dependent total photo-absorption cross section to the nucleon anomalous magnetic moment. This sum rule represents an important ground to test our understanding of the spin structure of the nucleon. Recently the sum rule was extended to finite Q^2 by Chiral Perturbation Theory [6, 7]. These new theoretical developments have renewed the interest in the very low momentum transfer region. At present the generalized GDH integral has been studied at JLAB for $Q^2 > 0.1$ GeV^2, while no measurements are available in region where χPT is applicable.

We propose to measure the polarized inclusive electron-proton cross section to derive the Q^2 dependence of the Gerasimov Drell Hearn sum rule in the very low momentum transfer region ($Q^2 < 0.05$ GeV^2) to test χPT predictions. In the same kinematics we will extract the structure function g_1 and its moments.

This proposal is organized as follows: in section 2 and 3 we will introduce the Gerasimov-Drell-Hearn Sum rule, its extension to finite momentum transfer, and we will discuss the extraction of the proton structure function g_1 and the derivation of its moments; in section 4 we will describe the proposed measurement and the experimental setup; finally in section 5 we will discuss the beam time request.

2 Physics Motivation

2.1 The Gerasimov-Drell-Hearn Sum Rule

The GDH sum rule was derived in 1966 independently by S. Gerasimov, and S. D. Drell and A. C. Hearn [2, 3]. It relates the helicity dependent total absorption cross section of circularly polarized photon on linearly polarized nucleons to the nucleon anomalous magnetic moment:

$$\int_{thr}^{\infty}(\sigma_{1/2}-\sigma 3/2)\frac{d\nu}{\nu}=-2\pi^2\alpha\frac{\kappa^2}{M^2} \tag{1}$$

where $\sigma_{1/2}$ and $\sigma_{3/2}$ are the total cross sections in the helicity 1/2 and 3/2 states, ν is the photon energy, κ is the nucleon anomalous magnetic moment, and M is the nucleon mass. The integration over the photon energy goes from the pion threshold to infinity.

The sum rule follows from unsubtracted dispersion relations applied to the forward Compton scattering amplitude and the Low Energy Theorem. The use of unsubtracted dispersion relations follows from causality, while the low energy theorem comes from gauge invariance and relativity. The generality of these assumptions suggests that the sum rule should be verified. Because of the $1/\nu$ weight in the integral, the sum rule is mostly sensitive to the low energy part of the photoabsorption cross section, i.e. the region where baryon resonances dominate and single pion production is the main contribution.

Presently the sum rule is being studied using circularly polarized photon beams at Mainz and Bonn [4, 5], while further measurements are planned at LEGS [8], Grenoble [9], and JLAB [10, 11]. At variance with the real photon case, where to measure the total photoabsorption cross section it is necessary to cover the full solid angle detecting both charged and neutral particles, inclusive electron scattering experiments at very low Q^2 allow the measurement of the total cross section by simply detecting the scattered electron. While measurements at $Q^2=0$ test the basic ingredients that enter in the derivation of the GDH sum rule, measurements of the small Q^2 regime test the dynamic behavior and the spin response of the nucleon at large distances.

2.2 The Generalized GDH Sum Rule

Recently a theoretically consistent generalization of the GDH integral at finite Q^2 was proposed by X. Ji and J. Osborne [6], relating the nucleon structure function $G_1=M^2g_1/\nu$ with the invariant photon-nucleon Compton scattering amplitude S_1 as follows

$$\bar{S}_1(0,Q^2)=4\int_{Q^2/2M}^{\infty}G_1(\nu,Q^2)\frac{d\nu}{\nu}, \tag{2}$$

where the overline on the Compton amplitude means that the elastic contribution has been subtracted. As pointed out by the authors of Ref. [6], this generalization of the GDH integral has the advantage of using well defined, invariant quantities, and of providing a well defined value for the integral at any momentum transfer value. Following this definition, it is possible to write the GDH integral as

$$I_{GDH}(Q^2)=8\pi^2\alpha\int_{Q^2/2M}^{\infty}G_1(\nu,Q^2)\frac{d\nu}{\nu}=\frac{16\pi^2\alpha}{Q^2}\int_0^1 g_1(x)dx. \tag{3}$$

For Q^2 values small compared with the nucleon mass, $S_1(0,Q^2)$ is computable in chiral perturbation theory giving a prediction for the behavior of the GDH integral in this region. Calculations have been performed by the authors of Ref. [6] and [7] at the order $\mathcal{O}(p^4)$ [1]. The experimental measurement of the GDH integral would therefore be very important to test and constrain such calculations. As pointed in Ref. [12] the range of applicability of the chiral expansion for individual isospin channel may be limited to $Q^2 < 0.05$ GeV^2 because of the contribution of the $\Delta(1232)$ resonance as well as of higher mass excited states. To perform an accurate test of chiral predictions it is therefore necessary to reach very low momentum transfers, of the order of $0.01 - 0.05$ GeV^2. The contribution of the $\Delta(1232)$, as well as the other isospin 3/2 resonances, would disappear if one considers the difference of the GDH integral for the proton and neutron. In this case the applicability of chiral theory may be extended to a somewhat larger Q^2. On this regard we would like to remind that the measurement of the GDH integral on the neutron down to $Q^2 \sim 0.02$ GeV^2 is the subject of the approved proposal E97-110 in Hall A [13]. A measurement of the integral for the proton covering the same Q^2 range would be very important to complete these studies.

Predictions on the Q^2 dependence of the GDH integral are also given by various phenomenological models. The model of Burkert and Ioffe [14] is based on a VMD parameterization of the non-resonant background originally proposed by Anselmino et al. [15] with the addition of resonance contributions as estimated from unpolarized data. This model indicates a strong contribution of the $\Delta(1232)$ resonance which explains the negative value of the GDH integral at the photon point and predicts a raise of the integral at low Q^2. A different approach was followed by Soffer and Teryaev [16] who assumed the validity of the Burkardt-Cottingham sum rule and the continuity of the integral $\int (g_1 + g_2)dx$ to derive the Q^2 dependence of the GDH integral. A comparison of the behavior predicted by these models as well as the prediction given by chiral perturbation theory is shown in Fig. 1. A high precision measurement of the GDH integral in the shown Q^2 range would allow to test these predictions and identify the mechanisms ruling the nucleon spin structure in this kinematics.

2.3 Higher moments of the spin dependent cross section

The GDH sum rule comes from the first term of the low energy expansion of the forward Compton amplitude

$$g(\nu) = -\frac{e^2\kappa^2}{8\pi M^2}\nu + \gamma_0\nu^3 + \mathcal{O}(\nu^5). \tag{4}$$

Based on the same assumption of the GDH sum rule, it is possible to define a second sum rule starting from the second term of the expansion $\gamma_0\nu^3$. The forward spin polarizability γ_0 can be in fact related to the third moment of the total cross section helicity difference as

$$\gamma_0 = -\frac{1}{4\pi^2}\int_{thr}^{\infty}\frac{\sigma_{1/2} - \sigma_{3/2}}{\nu^3}d\nu. \tag{5}$$

Because of the $1/\nu^3$ weighting, this integral converges more rapidly in energy than the GDH integral and therefore can more easily be determined by low beam energy measurements. For

[1] The former exploits the heavy baryon approximation while the latter is a relativistic baryon calculation.

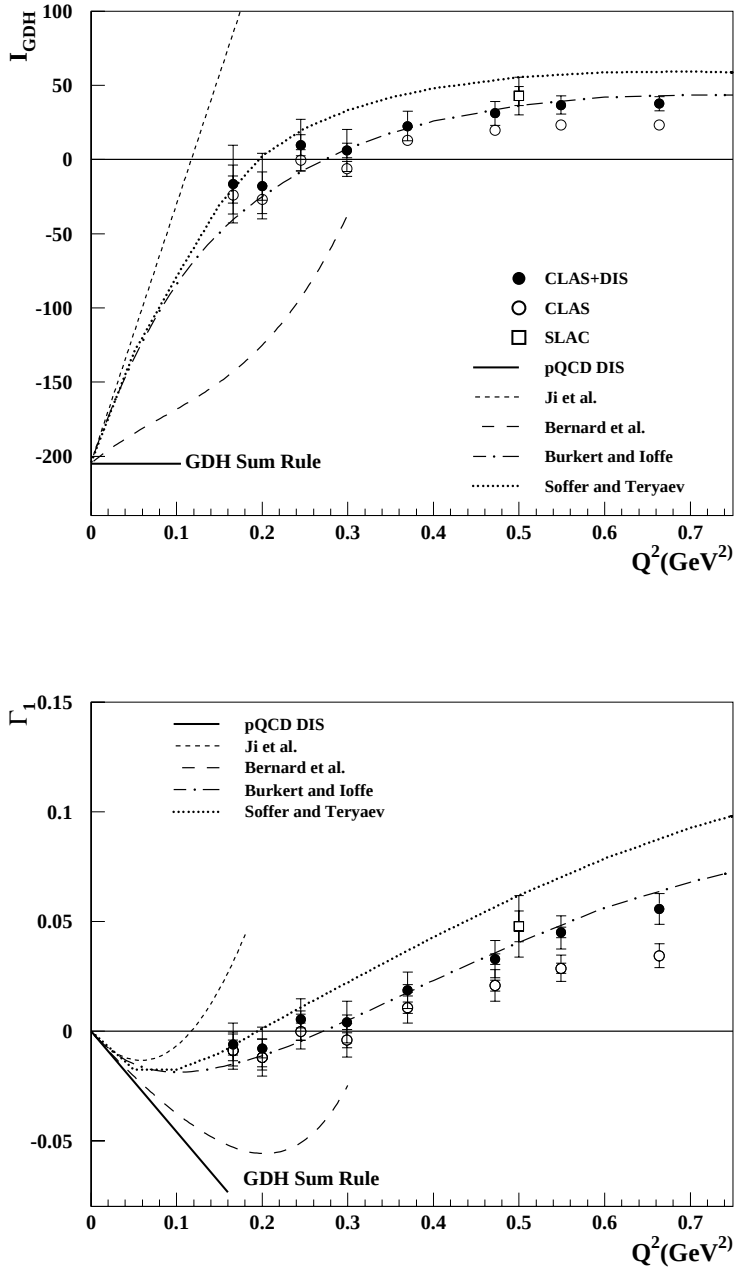

Figure 1: The Hall B preliminary results on the generalized GDH integral (top) and on the first moment of g_1 (bottom). The open circles are the CLAS data integrated over the measured region, while the full circles include the DIS contribution. The SLAC data (open squares) at Q^2 of 0.5 and 1.2 GeV^2 are shown for comparison. At large Q^2, the solid curve shows the pQCD evolution of the measured Γ_1 integral, while at low Q^2 the slope given by the GDH sum rule and chiral perturbation theory calculations of Ref. [6] and [7] are indicated (dashed and long dashed). The dashed-dotted and dotted lines are model predictions from Burkert and Ioffe [14] and Soffer and Teryaev [16].

the same reason it is also very sensitive to the low energy part of the cross section and in particular to the threshold behavior. A first evaluation of this sum rule at the photon point has been performed by the GDH experiment at Mainz, while no measurement at finite Q^2 exist [17]. A comparison with a phenomenological model is shown in Fig. 3. A Chiral perturbation theory calculation has also been performed recently [18]. The measurement of this observable could be performed at low momentum transfer using the same technique proposed for the GDH integral. This would provide the first measurement of this quantity at finite Q^2, where low energy theories can be applied.

2.4 Spin Structure Functions and Moments

The polarized inclusive electron-nucleon cross section can be expressed in terms of the spin structure function g_1 and g_2 as

$$\frac{d\sigma^{\rightarrow\Leftarrow}}{dE'd\Omega} - \frac{d\sigma^{\rightarrow\Rightarrow}}{dE'd\Omega} = \frac{4\alpha^2}{Q^2}\frac{E'}{ME\nu}\left[(E + E'cos\theta)\, g_1\left(x, Q^2\right) - 2Mxg_2\left(x, Q^2\right)\right] \tag{6}$$

where E and E' are respectively the incoming and outgoing electron energy. The measurement of this cross section gives direct access to the spin structure functions and in particular to g_1. In the parton model this structure function reflects the polarization of the quarks inside the nucleon and is therefore a fundamental quantity. In particular its first moment

$$\Gamma_1(Q^2) = \int_0^1 g_1(x, Q^2)dx \tag{7}$$

is connected to to the total spin carried by quarks. Γ_1 can be related to the generalized GDH integral defined in eq. 3, being

$$\Gamma_1 = \frac{Q^2}{16\pi^2\alpha} I_{GDH}. \tag{8}$$

For intermediate and large Q^2, perturbative QCD and the Operator Product Expansion can be used to evaluate Γ_1. At low Q^2, Γ_1 is predicted by chiral theories. In addition Γ_1 as well as the higher moments of g_1 are calculable quantities in the framework of lattice QCD. Therefore the experimental measurement of the structure function g_1 and of its moments would have high relevance for the study of the nucleon structure and for the test of fundamental theoretical predictions (see Fig. 1).

Evaluation of the moments of a nucleon structure function f from experimental data implies performing an integral over the whole x range at constant Q^2:

$$M_n(Q^2) = \int_0^1 dx x^{(n-1)} f(x, Q^2)\ . \tag{9}$$

Integration at constant Q^2 is especially important at low Q^2, where rapidly changing nucleon excited state form-factors ($1/Q^4$ or $1/Q^6$) give the most relevant contribution to the moments. This is true in particular for higher moments, being very sensitive to the resonance region (x >0.1). Actually, the data taken on a classical small acceptance spectrometer cover an interval in W at fixed electron scattering angle. As an example, Fig. 2 shows the kinematic

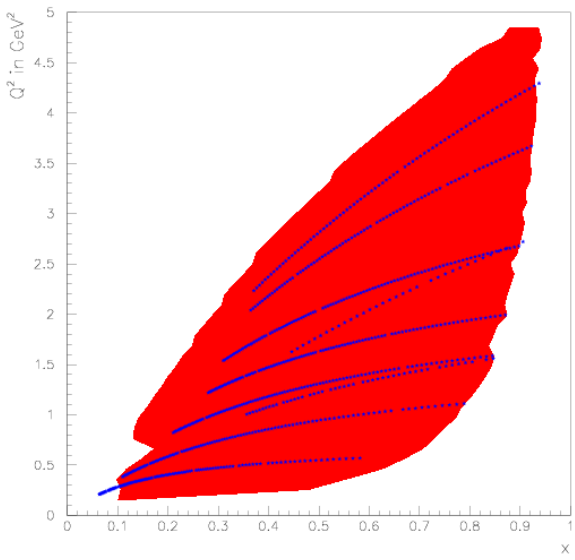

Figure 2: Kinematic range in Q^2 versus x for Hall C (points) and Hall B (red area) for the measurement of the F_2 structure function.

coverage for the CLAS detector and for the Hall C spectrometers in the case of the F_2 structure function measurement. The spectrometer data have to be interpolated, introducing further systematic uncertainties. On the contrary, no such interpolation is necessary with CLAS.

3 Experimental Setup and Proposed Measurement

3.1 Previous CLAS Experiments

A spin physics program with polarized beams and targets is active since a few years at JLAB. In particular, beam-target asymmetries in inclusive electron scattering on the proton and deuteron have been measured in the experiments E91-023 [20] and E93-009 [21]. They rely on the measurement of the inclusive double polarization asymmetry for longitudinally polarized electron and nucleon:

$$A_{||} = \frac{\sigma^{\rightarrow\Leftarrow} - \sigma^{\rightarrow\Rightarrow}}{\sigma^{\rightarrow\Leftarrow} + \sigma^{\rightarrow\Rightarrow}} = D\left(A_1 + \eta A_2\right) \tag{10}$$

where η and D are kinematics coefficients, the latter involving the ratio $R = \sigma_L/\sigma_T$, while $A_{1,2}$ are given by

$$A_1 = \frac{\sigma_{1/2} - \sigma_{3/2}}{\sigma_{1/2} + \sigma_{3/2}} \qquad A_2 = \frac{\sigma_{LT}}{\sigma_{1/2} + \sigma_{3/2}}. \tag{11}$$

These two quantities are related to the spin structure function g_1 and g_2 as

$$g_1\left(x,Q^2\right) = \frac{Q^2}{Q^2+4M^2x^2}\left[A_1\left(x,Q^2\right) + \frac{2Mx}{\sqrt{Q^2}}A_2\left(x,Q^2\right)\right]F_1\left(x,Q^2\right)$$
$$g_2\left(x,Q^2\right) = \frac{Q^2}{Q^2+4M^2x^2}\left[\frac{\sqrt{Q^2}}{2Mx}A_2\left(x,Q^2\right) - A_1\left(x,Q^2\right)\right]F_1\left(x,Q^2\right). \quad (12)$$

where F_1 is the unpolarized structure function. Due to the kinematics of these experiments, g_1 dominates $A_{||}$, and therefore can be extracted from the measured asymmetry ("asymmetry method"), provided an estimate for the unpolarized structure function F_1, the longitudinal-transverse ratio R, and the spin structure function g_2. The g_1 structure function, the generalized GDH integral, and Γ_1 were measured for $Q^2 = 0.17 - 1.25$ GeV^2 using this technique. Preliminary results from a first run completed in 1998 are shown in Figure 1 [22]. This measurement provided the first precise determination of the first moment of $\Gamma_1^p = \int g_1(x,Q^2)dx$ over an extended range at small and intermediate Q^2. However, the results are affected by significant systematic errors that dominate over the statistical uncertainty. One of the main contribution to the systematic uncertainty comes from the parameterization of the unpolarized structure functions F_1 and the longitudinal-transverse ratio R. While the structure function F_1 has been studied in great detail from moderate to large Q^2, no measurements exist for Q^2 below 0.1 GeV^2. A new set of data recorded in 2000 and presently under analysis should extend the existing results down to $Q^2 \sim 0.05$ GeV^2. However also in this case the extraction of g_1 will be performed using the "asymmetry method", and will be affected by similar systematics as discussed above. In fact, to reach these very low Q^2 values the CLAS detector was run in outbending configuration, i.e. with a magnetic field polarity for which electrons are bent away from the beamline. As we will discuss in section Sec. 3.5, the electron detection efficiency in this case is strongly reduced due to the particular optics of the CLAS Cherenkov Counter which was designed for the inbending field. For this reason the "asymmetry method", that is minimally affected by the electron efficiency, was generally adopted, leading however to significantly larger systematic uncertainties than the absolute cross section difference. Actually, attempts of extracting the absolute cross section difference are underway but only for the inbending field [23].

3.2 Proposed New Measurement

We propose a direct measurement of the inclusive spin dependent cross section with linearly polarized beam on a longitudinally polarized proton target for $Q^2 = 0.01 - 0.5$ GeV^2. This measurement will provide an accurate estimate of the generalized GDH integral, the structure function g_1, and its moments. The proposed kinematics extends the existing measurements to the region of applicability of Chiral theories and low energy expansion, providing the tool to experimentally test these predictions as well as other phenomenological models. In addition the minimum Q^2 is low enough to allow the evaluation of the GDH sum rule by extrapolating to the photon point.

In order to perform an absolute cross section measurement, we plan to use a modified setup installing a new Cherenkov Counter specifically designed for the outbending field configuration which is necessary to reach such low Q^2. This new detector will have a very high electron

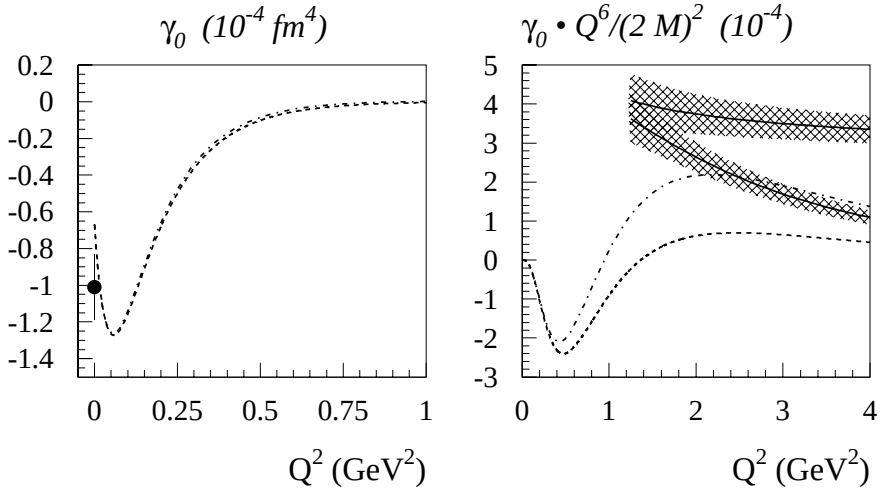

Figure 3: Q^2 dependence of the spin polarizabilities γ_0 (left) and of $\gamma_0 Q^6/(2M)^2$ (right) for the proton from Ref. [17]. The dashed and dashed-dotted lines represent phenomenological estimates, while the solid lines is the extrapolation from the DIS structure function [19].

detection efficiency (of the order of 0.999) to allow the measurement the absolute cross section with minimal corrections and a high pion rejection rate (of the order of 10^{-3}). The other components of the CLAS detector will be in the standard configuration.

We will use the $^{15}NH_3$ polarized target built for the previous CLAS polarization measurements [24]. This target exploits the Dynamical Nuclear Polarization technique (DNP) to polarize the material which is maintained in a liquid helium bath at 1 K and in a 5 Tesla longitudinal field. ^{15}N has the advantage that only one unpaired proton can be polarized, while all neutrons all paired to spin zero. This system operated successfully in the previous CLAS runs, providing typical proton polarization of the order of 75%. The material polarization will be monitored online by a NMR system [25] and then extracted offline by the analysis of elastic scattering events which are recorded simultaneously with the inelastic events thanks to the large acceptance of the CLAS detector. This method provides very precise values of the products of the beam and target polarization which is necessary for the evaluation of the GDH integral [24]. Being the elastic cross section very large at these low momentum transfers, the extraction of the beam-target polarization can be done using small data samples. In fact, even an on-line monitor of this quantity can be realized, as done during the CLAS previous run. The polarized target will be retracted by 1 m upstream to the CLAS center. This will increase the acceptance at low Q^2 by reducing the minimum angle for the scattered electron, allowing to reach $Q^2 = 0.01$ GeV^2. The target will contain a ^{12}C cell and an empty cell in addition to the NH_3 one for background measurements: each of these cells can be moved on beam by a remotely controlled system. In addition we will use a ^{15}N solid target already used in the previous measurements to check the nitrogen contribution. The NH_3 cell will be 1 cm

long, 1.5 cm in diameter and will contain approximately 1 cm^3 of frozen pellets.

We will exploit the highly polarized JLAB electron beam. Previous experiments have shown that a typical polarization of 70% can be expected. Beam currents in the range of 1-4 nA will be used for the proposed measurement. In these conditions, no significant heating of the target material takes place. The beam will be rastered over the target surface to minimize radiation effects, using the existing rastering equipment. Due to the low beam current and the rastering, radiation damage to the target material will be limited, and annealing will be required only once per week, thereby miminizing the target maintenance overhead. The beam polarization will be measured by the Hall B Möller polarimeter, while as mentioned above the final value of the product of beam and target polarization will be extracted by elastic events.

3.3 Extraction of the g_1 Structure Function

The structure function g_1 will be extracted from the difference of the inclusive cross section for antiparallel and parallel electron-proton spins as shown in Eq. 6. For $Q^2 < 0.1(GeV/c)^2$, and for incoming and outgoing electron energies of the order of the 1 GeV, i.e. small values of the Bjorken x, the kinematic coefficient $2Mx$ of the term linear in g_2 is a few percent of the coefficient $E + E'cos\theta$ of the term linear in g_1. This suggests that the cross section difference is dominated by g_1, which will allow a direct extraction of this quantity from the experiment. To quantify the g_2 contribution, we calculated the ratio of the two terms $2Mxg_2$ and $(E + E'cos\theta)\, g_1$, using a specific parameterization of g_1 and g_2 [26], based on available data, including the recent measurements from JLAB, HERMES, and SLAC. The estimated ratio

$$\frac{c_2}{c_1} = \frac{2Mxg_2}{(E + E'cos\theta)\, g_1} \tag{13}$$

is shown in Fig. 4 for various beam energies and for two values of the momentum transfer $Q^2 = 0.01$ GeV^2 and $Q^2 = 0.05$ GeV^2 as a function of Bjorken x.

We found that indeed, for the lowest momentum transfer considered, $Q^2 = 0.01$ GeV^2, the term proportional to g_2 is less than 2% of the observable under consideration, and rises to few percent at $Q^2 = 0.05$ GeV/c^2. This means that the g_2 contribution is negligible at the lowest Q^2, while small corrections may be necessary at higher Q^2, however with a very limited effect on the extraction of g_1, as discussed in section 4.2.

3.4 Kinematics and Monte Carlo Simulations

As already mentioned, the proposed experiments requires the coverage of the very low Q^2 region. This can be achieved by detecting electrons at small polar angle. While the minimum angle in the inbending configuration is $\sim 10 - 12^\circ$, a minimum angle of $\sim 7 - 8^\circ$ was reached running in outbending configuration in the previous polarization experiments. To further decrease the minimum angle, we propose to retract the target by 1 m and run with outbending field.

The exact kinematic coverage was studied performing Monte Carlo simulations using the standard code GSIM [27] developed for the CLAS detector. The purpose of our simulations was to assess the feasibility of the proposed measurement, with particular regard to the kinematic

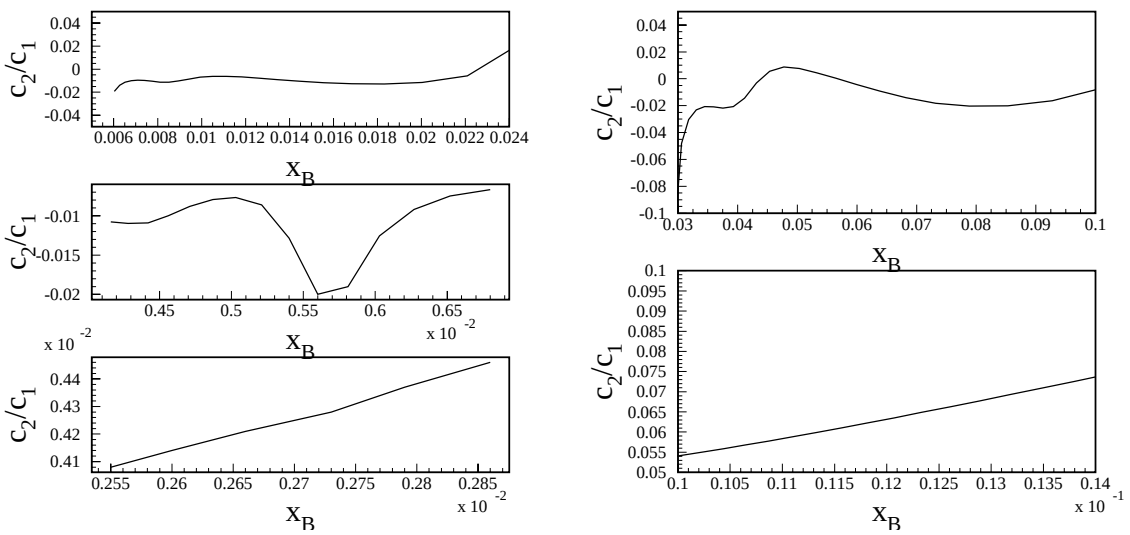

Figure 4: Ratio between the g_2 and g_1 term of the spin dependent cross section for $Q^2 = 0.01$ GeV^2 (left) and beam energy of 1.1, 1.6 and 2.4 GeV (top to bottom), and for $Q^2 = 0.05$ GeV^2 (right) and beam energy of 2.4 GeV and 3.2 GeV (top to bottom).

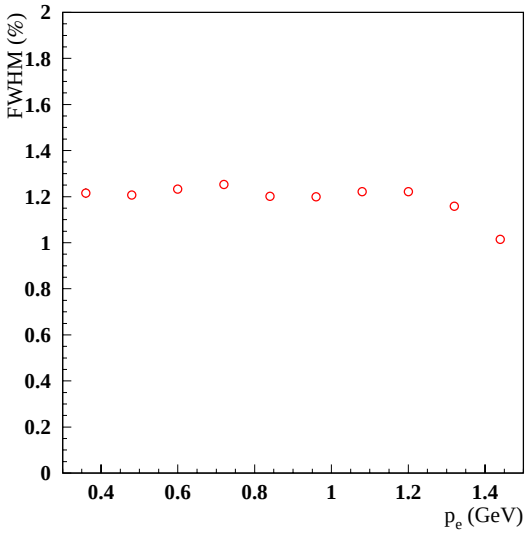

Figure 5: Electron momentum resolution with the proposed experimental setup.

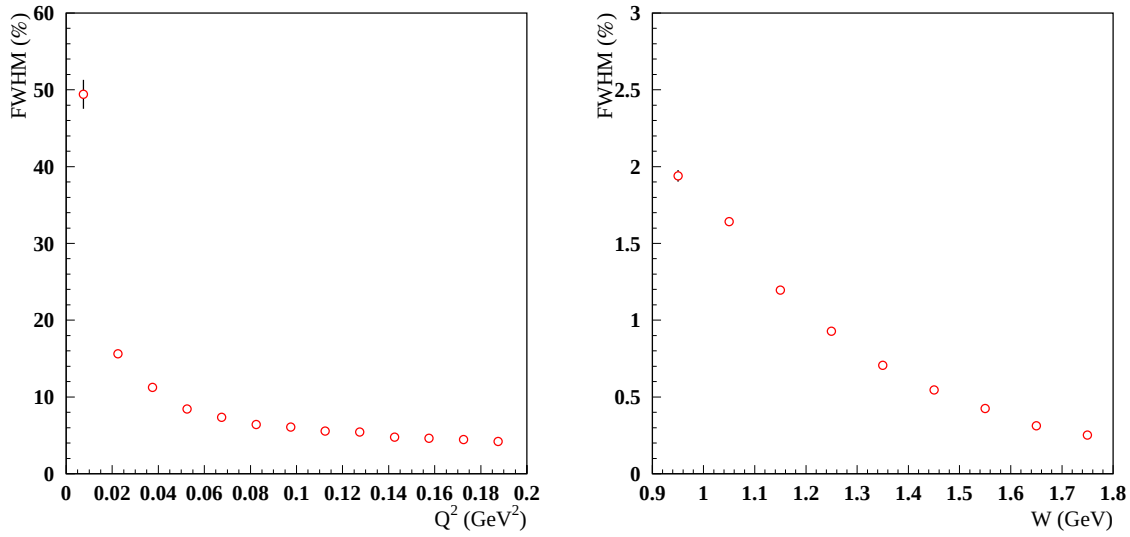

Figure 6: Q^2 and W resolution (assuming E_{beam} = 1.6 GeV) with the proposed experimental setup.

limits given by forward mechanical constraints such as those due to the beam pipe, torus magnet support structures, etc.

The inclusive measurement we propose requires that only the electron be detected. The electrons were generated according a phase space distribution, from a target one meter upstream, with four different beam energies (1.1, 1.6, 2.4, and 3.2 GeV). The polarized target effects were included in the simulations: the strong magnetic field and the geometrical acceptance were realistically taken into account. To extend the Q^2 range to very low values, the torus magnetic field was set such that the negative charges were bent away from the beam pipe (outbending field); the field strength was chosen in order to optimize the momentum resolution and the CLAS acceptance (0.4 B_{Max} at E_{Beam}= 1.1, 1.6 GeV and 0.6 B_{Max} at E_{Beam}= 2.4, 3.2 GeV). Fig. 5, and 6 show the momentum resolution and its effect on Q^2 and W with the experimental set-up corresponding to a beam energy of 1.6 GeV. We chose our binning according to the resolution obtained.

The MC events passed trough GSIM were then analyzed using the standard reconstruction code used to reconstruct the previous CLAS data of the previous polarization measurements. Fig. 7 shows the generated and the reconstructed electron polar angle: the proposed configuration allows to measure down to $\theta_{min} \sim 5^\circ$. The difference between generated and reconstructed yields is related to the limited azimuthal coverage of the CLAS detector. Fig. 8 shows the kinematic domain detectable at different beam energies: a wide range in Q^2 and W (0.01 GeV^2 < Q^2 < 1 GeV^2 and 1 GeV < W < 3 GeV) can be covered without discontinuity. This is of great advantage when calculating sum rules and moments, that need to be evaluated at constant Q^2.

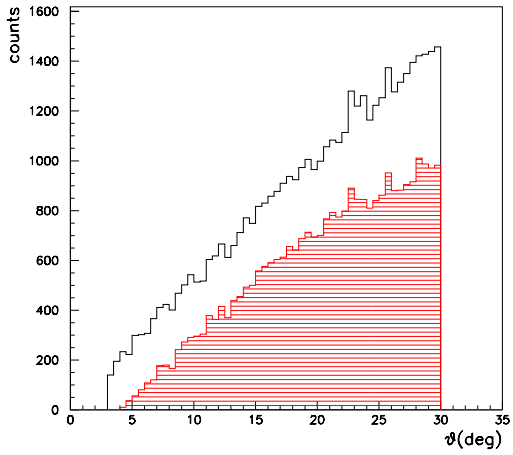

Figure 7: Generated and reconstructed electrons with the proposed experimental setup as a function of the electron polar angle. The ratio of reconstructed over generated events reflects the azimuthal coverage of the CLAS sectors. The minimum angle that can be reached is $\sim 5^{\circ}$.

3.5 Cherenkov Detector Design

3.5.1 The CLAS Cherenkov Detector

The present CLAS Cherenkov detector [28] was designed to maximize the azimuthal coverage in each of the six sectors of the detector up to an angle θ=45°. This was done by covering as much of the available space as possible with mirrors, and placing the light collecting cones and photomultiplier in the regions obscured by magnet coils. Each of the six sectors was divided in 18 regions of θ with two PMTs collecting the Cherenkov light. The optical elements of each module consist of two focusing elliptical mirrors, a 'Winston' light collection cone and a cylindrical mirror at the base of the cone. This complex geometry was chosen to compensate the effect of the CLAS toroidal field: the impact point of charged particles on the Cherenkov plane depends not only on the particle emission angle but also on the particle momentum. Consequently particle hitting the same point on the Cherenkov surface can have an angular spread up to 30°. The final Cherenkov design was therefore a compromise between the desired kinematic coverage and the system complexity. The optics, the geometry, the module positioning, and especially the mirror orientation were optimized for the low-rate, high-Q^2 experiments that use inbending electron tracks. In this configuration, the average track orientation of electrons entering the Cherenkov modules is reversed. The corresponding detection efficiency is strongly reduced because of the limited light collection and turns out to be quite non-uniform. Fig. 9 shows the Cherenkov counter performance with outbending magnetic field. The number of photoelectrons is strongly dependent on the angles of the scattered electron and shows a sizeable reduction in the middle of the sector and at forward polar angles. This characteristic indicates that in this regions the inefficiency for electron detection is significantly increased (up to 30%, according to our estimate) and the pion rejection rate is reduced. While in this condition it is still possible to identify electrons, the extraction of

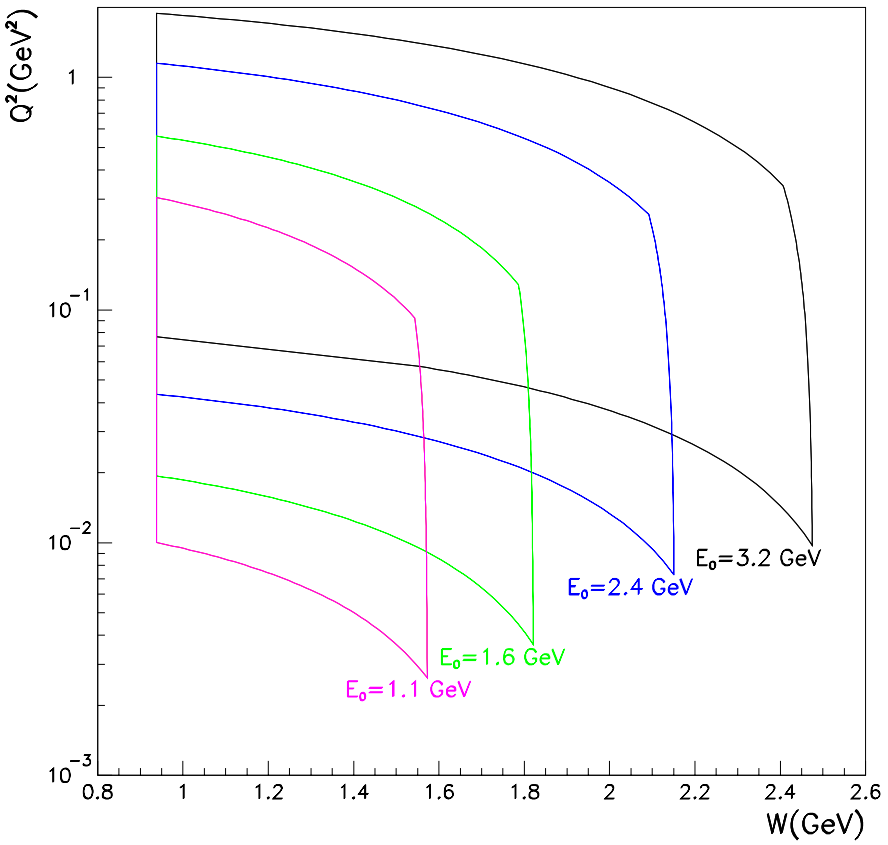

Figure 8: Kinematic coverage of the proposed experiment using four different beam energies. A minimum Q^2 of 0.01 GeV^2 can be reached. The minimum Q^2 covered by the existing CLAS data is ~ 0.05 GeV^2.

an absolute cross section would require large corrections which are difficult to be evaluated due to the complexity of the detector. On the other hand the proposed measurement requires high accuracy in the absolute electron yield normalization to keep the systematics as low as possible, and such large corrections would not be acceptable.

For these reasons we conclude that the proposed measurement requires the construction of a new Cherenkov detector specifically designed for the the detection of low Q^2, outbending electrons.

3.5.2 New Cherenkov Detector

We propose to instrument one sector of CLAS with a new Cherenkov counter replacing the existing one. We designed the new detector to fit the existing Cherenkov volume, such that no further modifications of CLAS will be necessary. Figure 10 shows a side view of CLAS with the new detector included: it is possible to see that indeed the new detector is compatible with the existing clearance. We plan to use the same radiator gas (C_4F_{10} - perfluorobutane) and the same gas flow control system used in the standard CLAS Cherenkov. C_4F_{10} has a high index of refraction (n=1.00153), which results in a high photon yield, and a pion momentum threshold of $p_\pi \sim 2.5GeV$, perfectly matched to the foreseen electron kinematic range. Due to the high electron rate at low Q^2, the ϕ coverage can be limited to the 40% of a sector ($\Delta\phi = \pm 12^\circ$) while still having a large counting rate [2]. On the contrary the polar coverage is maintained up to an angle θ=45° by implementing 15 modules each covering 2°.

The limited azimuthal coverage simplifies the module optical design: a good photon yield is obtained using a single reflection with a spherical mirror (R = 140 cm) and collecting the light onto a pair of 5" PMTs placed on the lateral sides. The geometry, the size, the mirror position, and dimensions as well as the the assembly of the 15 modules have been optimized for this experiment, using a dedicated FORTRAN code, while a complete GEANT simulation is underway. Figs. 11 and 12 show a schematic view of a single module of the new Cherenkov and its focusing properties. The average number of the collected photo-electron yield is shown in Fig. 13, assuming a mirror reflectivity ∼85% and a PMT quantum efficiency ∼14% [29] in the wavelength range 200-600 nm. It is clear how a very good uniformity as well as a high photoelectron yield ($< N_{phel} > \sim 20$) is obtained in the full angular range of our interest.

We foresee a maximum of two weeks for dismounting one module of the existing Cherenkov and installing the new one. On the other hand, a similar amount of time will be necessary for installing the polarized target, so that no additional shutdown will be requested. After the completion of the experiment proposed, during the two weeks necessary for removing the polarized target, the new Cherenkov module may be dismounted and the old one put back in place. This way the standard CLAS configuration may be restored, with minimal impact on the rest of the CLAS experimental program.

Funding for the construction of the Cherenkov Counter would be provided by the Italian National Institute for Nuclear Physics (INFN). We foresee a period of 18 months for the construction of this detector, including prototyping and testing. Our plans include a measurement at the CERN test beam [29] to calibrate the device in advance both in terms of efficiency and

[2] To be conservative, a $\Delta\phi = \pm 9^\circ$, corresponding to the minimum detection angle, was used in our counting rate estimate as mentioned in Section 3.6

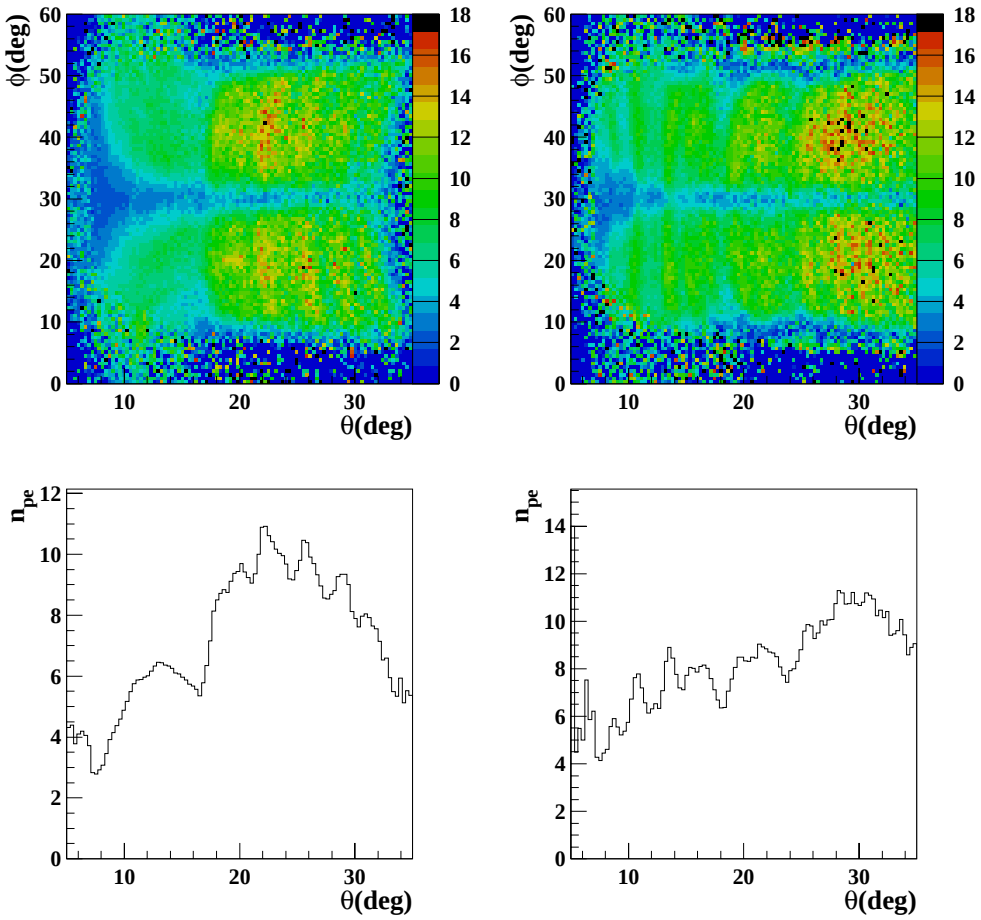

Figure 9: CLAS Cherenkov performance with outbending field. The average number of photoelectron is shown as a function of the electron angles for electron momentum of 0.6 GeV (left plots) and 1.5 GeV (right plots).

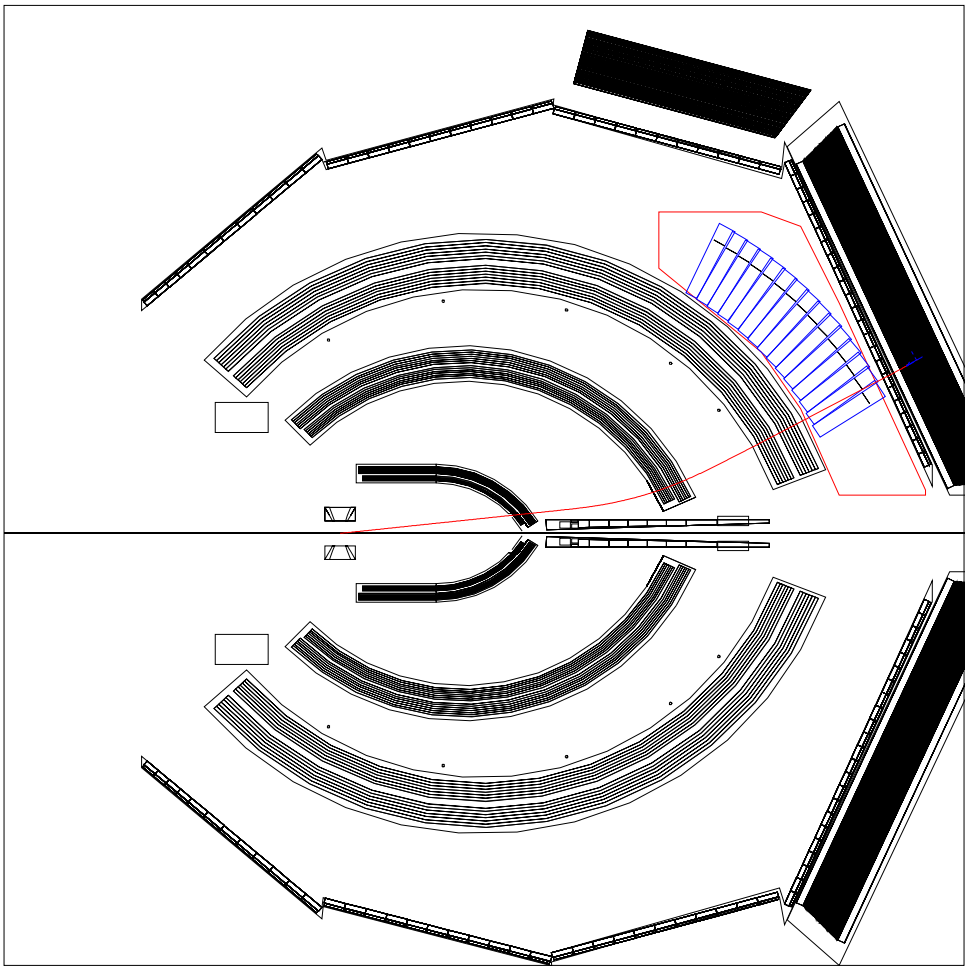

Figure 10: Side view of CLAS with the new detector included (upper part). The new Cherenkov (red) fits inside the existing volume (blue). The red track corresponds to an electron emitted at 6^o.

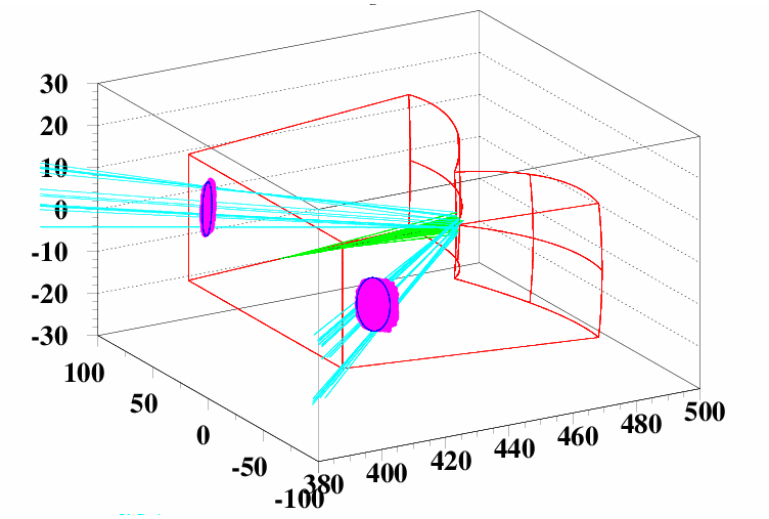

Figure 11: New Cherenkov single module 3D view. The circles correspond to the PMTs sensitive area. Only photons hitting the center of the module are drawn, while the side spots correspond to the intersection of all possible photon trajectories with the PMT sensitive area.

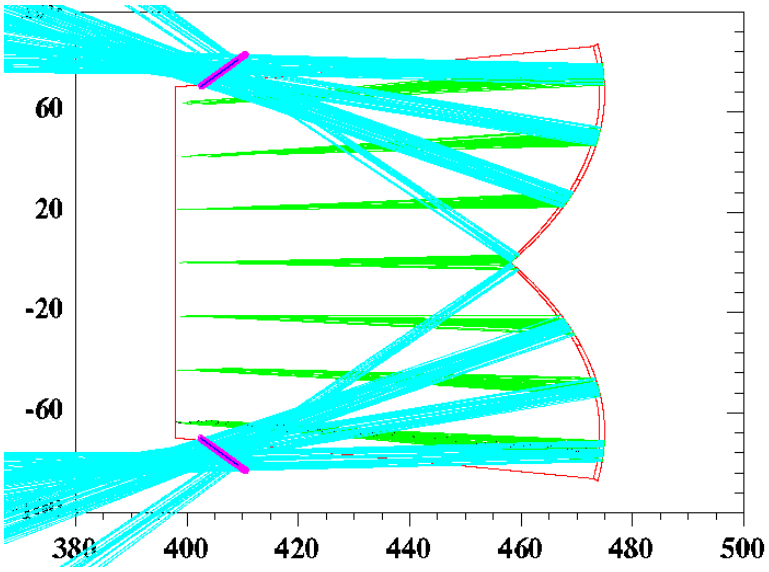

Figure 12: New Cherenkov focusing properties: electrons generated in different points with a wide angular spread are focussed into the same spot.

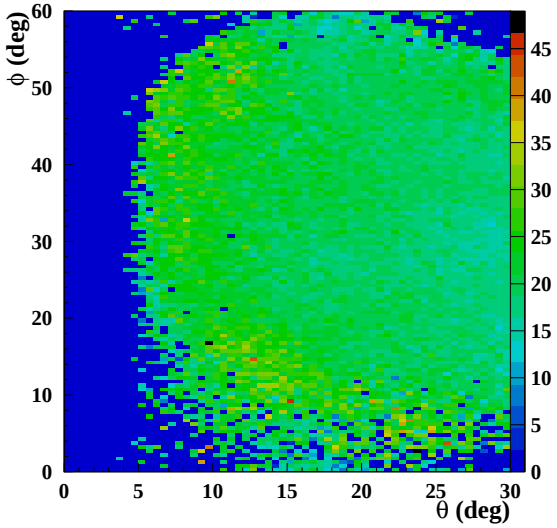

Figure 13: Simulated response of the new Cherenkov detector: the average number of photoelectrons is shown as a function of the electron angles.

pion rejection.

We want to remark that, with such a new detector inserted in CLAS, also a whole family of exclusive measurements at very low momentum transfer would be made possible, opening the possibility for a new specific experimental program.

3.6 Counting Rates and Statistical Accuracy

The expected counting rates for inelastic scattering were estimated assuming: a W bin of 20 MeV, a Q^2 bin of 0.01 GeV^2, a polar angular interval $\Delta\phi$ of 18^0 for one module of the Cherenkov detector, a beam current ranging from 1 to 2 nA depending on the energy, beam energies of 1.1, 1.6, 2.4 GeV and 3.2 GeV, and finally 4 days of beam time at 1.1, 1.6 GeV and 7 days at 2.4 GeV, 3.2 GeV. Based on the kinematic constraints discussed in the previous sections, we assumed a minimum electron detection angle of 5 degrees. A minimum energy for the outgoing electron of 300 MeV was also assumed in integration to obtain the GDH sum rule. The unpolarized inclusive electron scattering cross section $\frac{d\sigma}{dWdQ^2}$ was calculated based on a parameterization of the two structure functions F_1 and F_2 [26] as

$$\frac{d\sigma}{dWdQ^2} = \frac{4\pi\alpha^2 E^{'} W cos^2(\theta/2)}{Q^4 M E}\left[\frac{2}{M} tan^2(\theta/2) F_1(x) + \frac{Q^2}{\nu} F_2(x)\right] \tag{14}$$

As examples the projected counts from the inelastic cross section for Q^2=0.01 and 0.05 GeV^2 are shown in Figure 14.

Using the parameterization of g_1 from Ref. [26] and the above estimated counting rates, we evaluated the statistical errors. The results are reported in Fig. 15. Projected errors bars

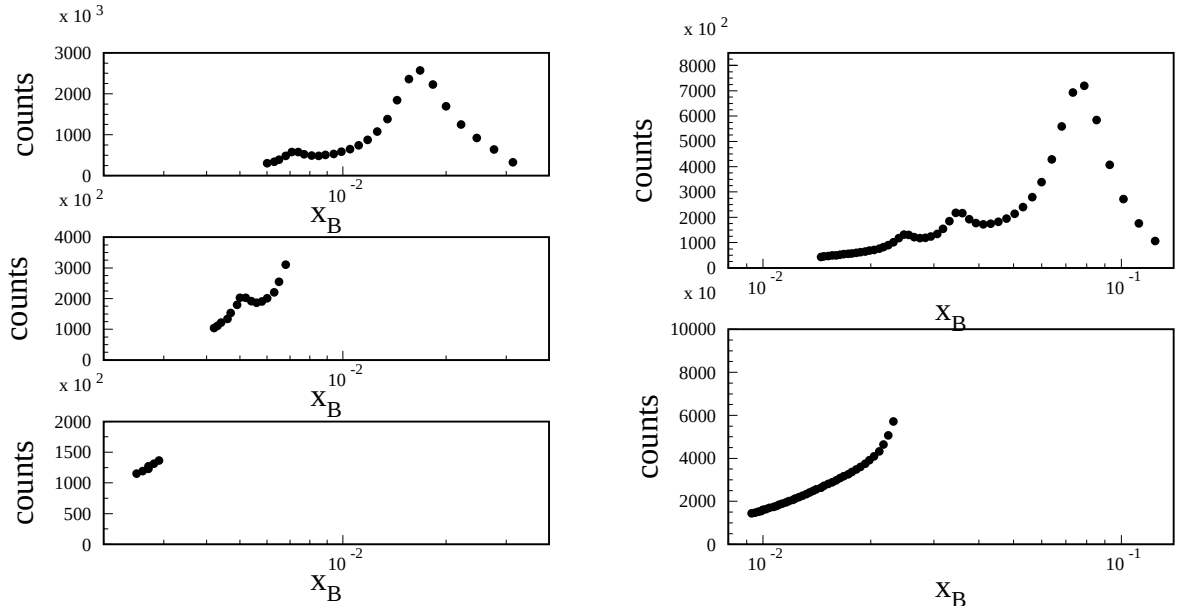

Figure 14: Expected counts from inelastic events for $Q^2 = 0.01$ GeV^2 at a beam energy of 1.1, 1.6 and 2.4 GeV (left panels, top to bottom), and for $Q^2 = 0.05$ GeV^2 at a beam energy of 2.4 and 3.2 GeV (right panels, top to bottom).

for the generalized GDH sum rule and for the Γ_1 integral are shown in Figure 18.

We also calculated the rate of elastic and quasi-elastic scattering off NH_3, which is the dominant process at our lowest Q^2. We found that with the proposed luminosity the rate at the smallest detection angles (5-6^o) is of the order of 2 kHz, therefore compatible with the current DAQ capability. The CLAS resolution is sufficient to separate this background during the off-line analysis.

4 Systematic Errors

The extraction of the spin structure functions is affected by two types of systematic errors. The first is of instrumental origin, that is

- Electron efficiency
- Beam and target polarization
- ^{15}N background
- Beam charge asymmetry
- Luminosity and filling factor

The second is related to the model assumptions required to extract the desired observable, that is

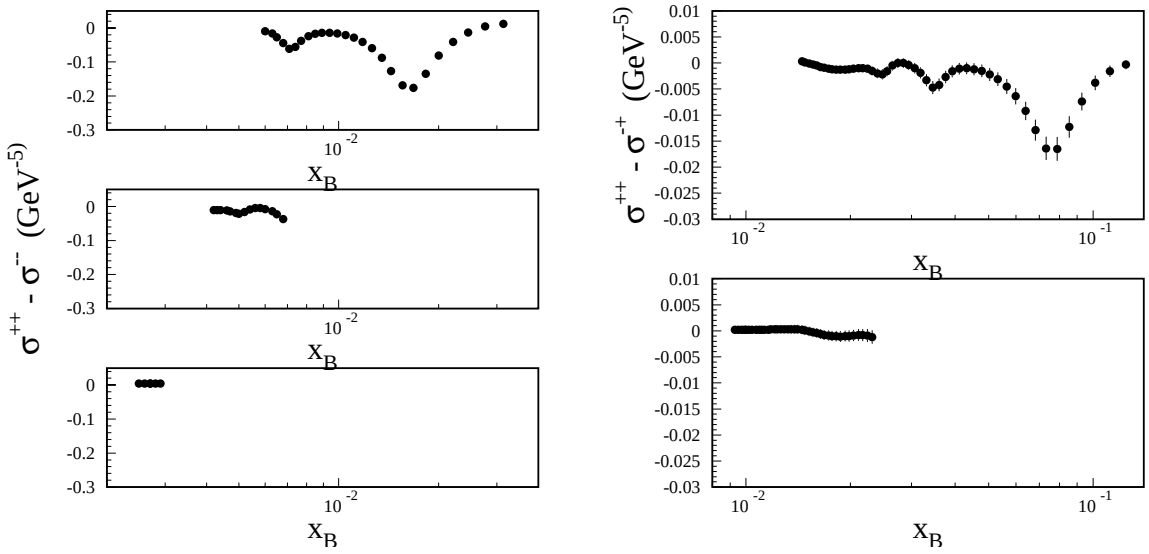

Figure 15: Estimated statistical accuracy for the polarized cross section difference for $Q^2 = 0.01$ GeV^2 at a beam energy of 1.1, 1.6 and 2.4 GeV (left panels, top to bottom), and for $Q^2 = 0.05$ GeV^2 at a beam energy of 2.4 and 3.2 GeV (right panels, top to bottom).

- Modeling of g_2
- Extrapolation into the unmeasured kinematic region
- Radiative Corrections

4.1 Instrumental Systematics

As mentioned before, the new Cherenkov counter will be tested and calibrated using a test beam facility at CERN. The beam that we plan to use is a mixture of positrons, positive pions and protons, with energies in the JLAB range. An existing reference particle identification equipment will be used to cross-calibrate our detector. This test will therefore characterize the absolute electron detection efficiency and the hadron rejection. Furthermore, a full GEANT-based simulation of CLAS will be performed to evaluate the overall reconstruction efficiency. During operation with CLAS, we will also be able to extract the absolute cross section on hydrogen by comparing the measurements on NH_3 and ^{15}N, thereby providing a direct check of the absolute efficiency. We estimate not more than 5 % systematic error related to this procedure.

The product of the beam and target polarization will be extracted from the elastic double spin asymmetry which will be measured simultaneously with the inelastic events. In the proposed measurement, the kinematic conditions are such that the elastic beam-target asymmetry has a very weak dependence on the elastic form factors G_E, G_M. Indeed, according to the data analysis performed on the data from the EG1a running period, the corresponding uncertainty amounts to 1-2 % [30].

The contribution from the polarized proton in the ^{15}N can be evaluated based on existing measurements [31] and for a proton polarization of about 80 % it turns out to be about 10 %. Considering that only one proton from ^{15}N is polarized against 3 protons from H, assuming a 50 % uncertainty on the ^{15}N polarization, the resulting systematic error is about 1-2 %.

The beam charge asymmetry will be continuously monitored using three different types of current monitors available in Hall B, i.e. Faraday cup, a Synchrotron Light Monitor (SLM), and an Optical Transition Radiation Monitor (OTR) [32]. Typical values of such asymmetry are in the range 0.1-0.3 %. This measurement can be performed with a negligible systematic error. To further reduce false asymmetries, the target polarization will be periodically reversed during the experiment.

The so-called filling factor or packing fraction, that is the amount of NH_3 actually present in the target cell can be estimated by comparing measurements on empty target and ^{15}N cell. The resulting systematic error is not exceeding 3 %. The luminosity will be evaluated from the packing fraction and the accumulated charge, measured by the Faraday cup, therefore the corresponding error is already taken into account by the quoted 3 %.

4.2 Further Corrections and Assumptions

For the method we are proposing, based on the direct measurement of the cross section difference, the modeling error on the g_1 extraction is limited to the knowledge of g_2. We estimated the associated systematic error assuming a 100% uncertainty on g_2: practically, this was done assuming $g_2 = 0$ and re-extracting g_1 from the cross section difference calculated by using the parameterizations from [26]. We found that this systematic error is in the range 1-10 %, depending on Q^2.

An additional uncertainty is associated with the extrapolation into the unmeasured region. We obtained a conservative estimate of the corresponding systematic error by calculating the unmeasured part using the parameterizations from [26] and assuming a 50 % uncertainty on this correction. We found that this systematic error is in the range 2-10 %, depending on Q^2. Available data at the photon point as well as at finite Q^2 will in fact provide a more stringent constraint, thereby reducing this particular source of systematics.

The last correction to apply is coming from radiative effects. We calculated both elastic and inelastic internal corrections using a code based on Ref. [33]. The most prominent effect is the elastic radiative tail. Therefore we calculated such corrections using two different parameterizations of the proton elastic form factors [34, 35]. Picture 16 shows the comparison of the radiated cross sections obtained from these two parameterizations. Instead, picture 17 shows the ratio between the two radiated cross sections. From this ratio we evaluated the corresponding systematic error, which turns out to be of the order of 5%. In additional, exploiting the large kinematic coverage of CLAS and the capability of measuring both inelastic and elastic scattering, we expect that applying an appropriate iterative procedure it will be possible to reduce this error. External corrections will be taken care of by the GEANT-based simulation.

A summary of all systematic errors is reported in Table 1. Their sum in quadrature, referred to I_{GDH} and Γ_1 as a function of Q^2, is reported as a band in Figure 18.

Using the CLAS detector together with the proposed new Cherenkov counter, we will not need any interpolation procedure as all the kinematically allowed region will be measured

Table 1: Summary of all systematic errors on the Generalized GDH.

electron efficiency	< 5 %
beam and target polarization	1-2 %
^{15}N background	1-2 %
beam charge asymmetry	-
luminosity and filling factor	3 %
modeling of g_2	1-10 % (depending on Q^2)
extrapolation	1-10 % (depending on Q^2)
radiative corrections	5 %

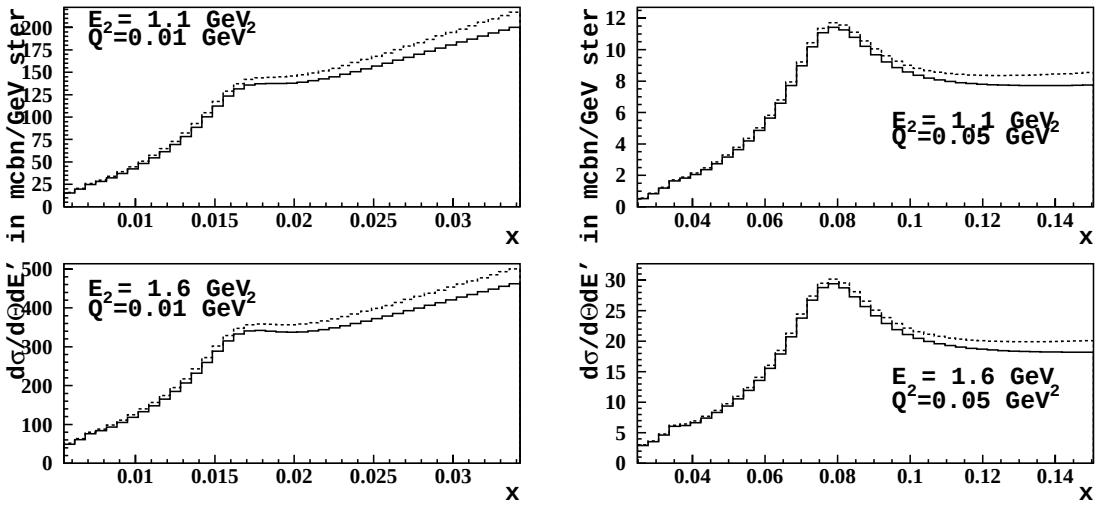

Figure 16: Estimated difference in radiative corrections due to different parameterizations of the elastic tail for the cross section on hydrogen at $Q^2 = 0.01$ GeV^2 and a beam energy of 1.1, 1.6 GeV (left panels, top to bottom), and for $Q^2 = 0.05$ GeV^2 and a beam energy of 1.1, 1.6 GeV GeV (right panels, top to bottom).

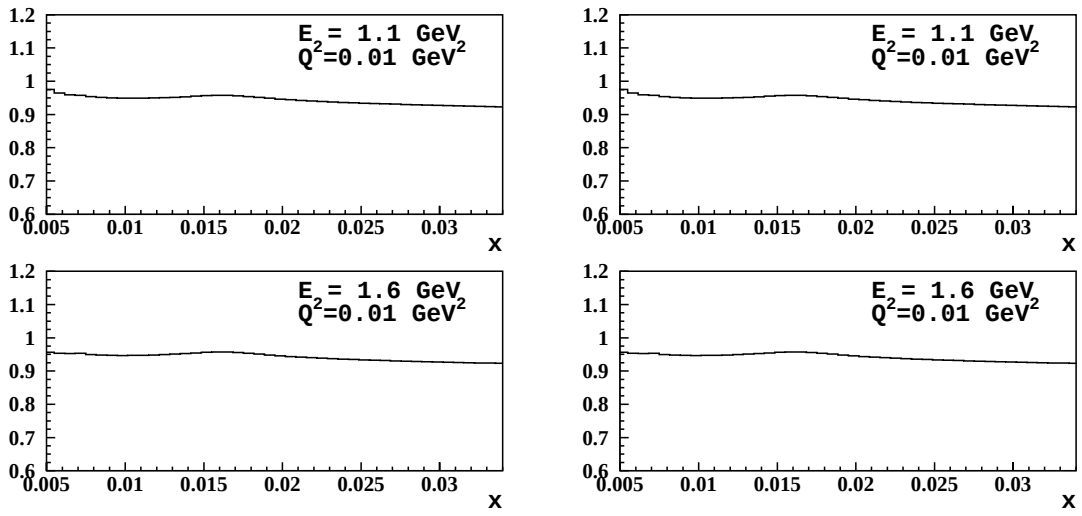

Figure 17: Estimated difference in radiative corrections due to different parameterizations of the elastic tail for the cross section on hydrogen at $Q^2 = 0.01$ GeV^2 and a beam energy of 1.1, 1.6 GeV (left panels, top to bottom), and for $Q^2 = 0.05$ GeV^2 and a beam energy of 1.1, 1.6 GeV GeV (right panels, top to bottom). The difference in this case is plotted as a ratio to indicate the associated systematic error.

Table 2: Comparison of the systematic errors on Generalized GDH due to model assumptions with asymmetry and cross section methods: the errors associated with the parameterization of F_1, R, g_2, and with the extrapolation of g_1 in the unmeasured region are reported.

Asymmetry Method					
Q^2 (GeV^2)	F_1 (%)	R (%)	g_2 (%)	Extrapolation (%)	total
0.2	26	8	6	11	30
0.1	18	4	2	2	19
0.05	20	4	2	3	21
0.01	38	2	3	12	41
Cross Section Method					
Q^2 (GeV^2)	F_1 (%)	R (%)	$g_2 = 0$	Extrapolation (%)	total
0.2	–	–	7	9	11
0.1	–	–	3	2	4
0.05	–	–	1	2	2
0.01	–	–	< 1	7	7

at once. This is particularly important when calculating the generalized GDH integral and higher moments of the structure functions.

4.3 Comparison with the Asymmetry Method

As mentioned in the previous sections, the extraction of the spin structure functions is presently being performed from the existing CLAS data using the the "asymmetry method". In this case, one needs to parameterize the quantities R, F_1 and g_2. This is introducing an additional systematic error with respect to the absolute cross section measurements we propose. To make a quantitative comparison of the systematics arising from these two methods, we estimated the error due to F_1 comparing the parameterizations of Ref. [36] and [37] for this structure function. The same was done for R using the parameterizations of Ref. [38] and [39], while for g_2 we applied the above described procedure. The comparison of the systematic errors for the two methods is reported in Table 2.

We conclude that with the proposed cross section measurement it will be possible not only to study the new range Q^2=0.01-0.05 GeV^2, but also to cover some of the previous measurements at the lowest Q^2 values, reducing the systematics by at least a factor 3.

5 Summary and Beam Request

We propose to study the spin response of the proton in inclusive scattering at very low momentum transfers Q^2=0.01-0.5 (GeV/c)^2, and thereby calculate the corresponding generalized GDH Sum Rule, extract the structure function g_1, and its moments.

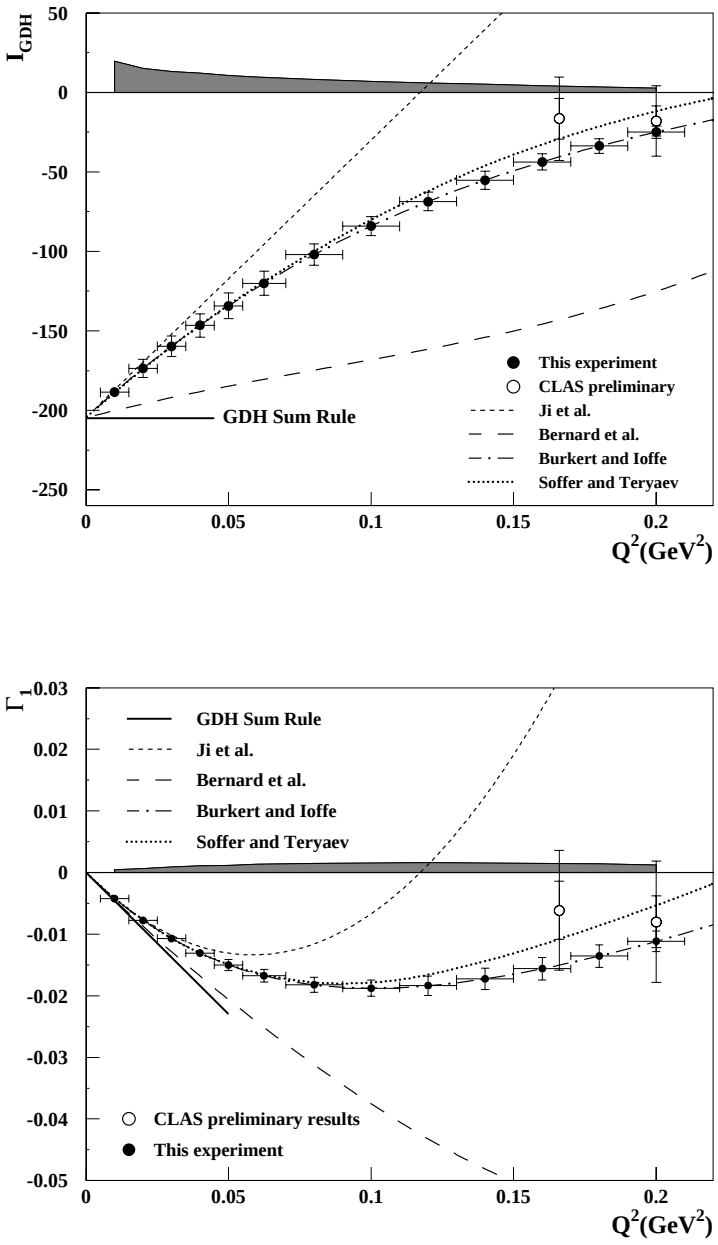

Figure 18: Projected results for the I_{GDH} and Γ_1 integrals. Full points are the expected results from the proposed experiment with statistical errors only. The open circle are the CLAS preliminary results presently available. The dark grey band shows the estimated systematic error with our proposed method. Chiral perturbation theory calculations of Ref. [6] and [7] are shown by short-dashed and long-dashed lines, while the model predictions from Burkert and Ioffe [14] and Soffer and Teryaev [16] are indicated by the dashed-dotted and dotted lines.

Table 3: Beam Request.

Energy (GeV)	days	current (nA)
1.1	4	1
1.6	4	1
2.4	7	1
3.2	7	2
Total	22	

Instead of relying on asymmetry measurements, our goal is to measure directly the cross section difference, which at the lowest momentum transfers is dominated by the structure function g_1. This way, the various sources and amounts of systematic errors would be reduced. This measurement will allow to understand the behavior of the Sum Rule at very low Q^2, where Chiral theories are applicable. This is an important aspect of our understanding of the proton structure in the non-perturbative domain.

As experimental method, we propose to build and install in CLAS one module of a new Cherenkov detector, optimized for very high and uniform efficiency at the very low angles required by the measurement. The already existing ammonia polarized target would be used as well in the experiment. In Table 3, we report our beam request at the various energies: a total of 22 days is requested. We foresee that from one to two weeks will be necessary to dismount one sector of the existing Cherenkov and install the new one. In the same period, the installation of the polarized target can take place. Given the need of testing the new equipment, we foresee that one week of commissioning time in addition to the beam time request will be necessary.

References

[1] For a recent review see: B. W. Filippone and X. D. Ji, hep-ph/0101224 (2001).

[2] S. B. Gerasimov, Sov. J. Nucl. Phys. **2**, 430 (1966).

[3] S. D. Drell and A. C. Hearn, Phys. Rev. Lett. **16**, 908 (1966).

[4] J. Ahrens *et al.*, Phys. Rev. Lett. **87**, 022003 (2001).

[5] T. Michel, in Proceedings of the 9^{th} *International Conference on the Structure of Baryons (Baryons 2002)*; Eds. C. Carlson and B. Mecking, World Scientific, Singapore (2003).

[6] X. D. Ji and J. Osborne, Phys. Lett, Phys. Lett. **B472**, 1 (2000); X. D. Ji *et al.*, J.Phys. **G27**, 127 (2001).

[7] V. Bernard *et al.*, hep-ph/0203167 (2002).

[8] A. Sandorfi, in Proceedings of GDH2002.

[9] J. P. Didelez, in Proceedings of GDH2002.

[10] JLab E91-015, Spokesperson D. Sober.

[11] JLab E94-117, Spokesperson J. P. Chen, S. Gilad, C.Whisnant.

[12] V. D. Burkert, Phys. Rev. **D63**, 097904 (2001).

[13] JLab E97-110, Spokesperson J. P. Chen, A. Deur and F. Garibaldi.

[14] V. D. Burkert and B. L. Ioffe, Phys. Lett. **B296**, 223 (1992); J. Exp. Theor. Phys. **78**, 619 (1994).

[15] M. Anselmino, B. L. Ioffe and E. leader, Sov. J. Nucl. Phys. **49**, 189 (1986).

[16] J. Soffer and O. V. Teryaev, Phys. Rev. Lett. **70**, 3372 (1993), Phys. Rev. **D51**, 25 (1995).

[17] D. Drechsel, B. Pasquini, and M. Vanderhaeghen, *in preparation.*

[18] C. W. Kao and M. Vanderhaeghen, *hep-ph/0209241*, Phys. Rev. **D** in press.

[19] J. Blümlein and H. Böttcher, Nucl. Phys. **B636**, 225 (2002).

[20] JLab E91-023, Spokesperson V. D. Burkert, D. G. Crabb and R. Minehart.

[21] JLab E93-009, Spokesperson S. E. Kuhn, G. E. Dodge and M. Taiuti.

[22] Renee H. Fatemi, PhD thesis, University of Virginia.

[23] R. Minehart, private communication.

[24] C. D. Keith *et al.*, accepted by Nuclear Instruments and Methods.

[25] G. R. Courth *et al.*, Nucl. Instr. and Meth. **A324**, 433 (1993).

[26] S. Kuhn, private communication.

[27] GSIM, *CLAS GEANT Simulation*, http://improv.unh.edu/Maurik/gsim_info.shtml.

[28] G. Adams *et al.*, Nucl. Instr. and Meth. **A465**, 415 (2001).

[29] M. Iodice *et al.*, Nucl. Instr. and Meth. **A411**, 223 (1998).

[30] R. De Vita *et al.*, Phys. Rev. Lett. **88**, 082001 (2002).

[31] D.G. Crabb *et al.*, Nucl. Instr. and Meth. **A356**, 9 (1995).

[32] V. Burkert *et al.*, CLAS note, CLAS-01-007.

[33] L. W. Mo and Y. S. Tsai, Rev. Mod. Phys. **41**, 205 (1969).

[34] P.E. Bosted *et al.*, Phys. Rev. **C51**, 409 (1995).

[35] S.I. Bilenkaya *et al.*, JETP Lett. **19**, 317 (1974).

[36] A. Bodek *et al.*, Phys. Rev. **D20**, 1471(1979); S. Stein *et al.*, Phys. Rev. **D12**, 1884 (1975).

[37] I. Niculescu, PhD Thesis, Hampton University 1999.

[38] G. Ricco *et al.*, Nucl. Phys. **B555**, 306(1999).

[39] L.W. Whitlow *et al.*, Phys. Lett. **B250**, 193 (1990).